NANO EXPRESS

Architectural Growth of Cu Nanoparticles Through Electrodeposition

Wen-Yin Ko · Wei-Hung Chen · Ching-Yuan Cheng · Kaun-Jiuh Lin

Abstract Cu particles with different architectures such as pyramid, cube, and multipod have been successfully fabricated on the surface of Au films, which is the polycrystalline Au substrate with (111) domains, using the electrodeposition technique in the presence of the surface-capping reagents of dodecylbenzene sulfonic acid and poly(vinylpyrrolidone). Further, the growth evolution of pyramidal Cu nanoparticles was observed for the first time. We believe that our method might open new possibilities for fabricating nanomaterials of non-noble transition metals with various novel architectures, which can then potentially be utilized in applications such as biosensors, catalysis, photovoltaic cells, and electronic nanodevices.

Keywords Copper · Shape control · Electrochemistry · Nanostructure · Nanoparticles

W.-Y. Ko · W.-H. Chen · K.-J. Lin (✉)
Department of Chemistry, Center of Nanoscience
and Nanotechnology, National Chung-Hsing University,
250, Kuo Kuang Rd.,
Taichung 402, Taiwan, ROC
e-mail: kjlin@dragon.nchu.edu.tw

W.-Y. Ko
e-mail: d9551108@mail.nchu.edu.tw

C.-Y. Cheng
Experimental Facility Division, National Synchrotron Research
Center, 101 Hsin-Ann Road, Hsinchu Science Park, Hsinchu
30076, Taiwan, ROC

Introduction

Shape control of metallic particles has been receiving tremendous attention due to their unique electronic, magnetic, optical, and catalytic properties; further, they have a wide range of applications, such as chemical- and bio-sensing, catalysis, photonics, and optoelectronics [1–7]. The fabrication of metallic nanostructures with controllable shapes is important for utilizing the shape-tunable properties of nanomaterials. Recently, non-noble copper nanostructures have received a significant interest for several reasons. First, copper nanostructures enhance the boiling surface: this can have considerable impact on the chemical/thermal processes applied to heat flux in Cu interconnects and semiconductor devices [8]. Second, the high stability of copper nanoparticles (NPs) makes them an attractive alternative to Ag and Au nanocolloids in low-cost applications such as ink-jet printing of flexible conductors and radio frequency identification (RF-ID) tags [9]. Third, face-centered cubic (*fcc*) copper with a full *d*-band is regarded as an ideal alternative material to nanomaterials because of its excellent electrical conductivity and catalytic properties [10–12].

Unlike the case of noble metals such as Ag and Au, shape-controlled non-noble transition-metal nanostructures have rarely been studied and reported because they get rapidly converted into oxides [13, 14]; this reduces the intrinsic characteristics of non-noble transition metals. A challenging problem is the development of effective methods to avoid the oxidation and corrosion of important non-noble metals. Solution-phase method using surface-modifying reagents is a common method for synthesizing non-noble metal NPs [15, 16]. Further, oxidation under ambient conditions can be prevented by using amphiphilic surfactant and graphene coating to blend water-based

copper nanocolloids into a polymer matrix [17]. However, the procedures for governing controllable shapes are often time-consuming and complicated, and the apparatus is expensive.

The electrodeposition method is a relatively inexpensive and simple technique in material synthesis, and it has been used as an alternative method for controlling the shapes of metal-based NPs such as Pd, Cu_2O, and Zn [18–20]. However, there have been very few reports on the shape control of metallic Cu by electrodeposition; only one or two shapes have been generated by altering the experimental parameters [21, 22]. In our previous study, we reported the successful synthesis of well-defined Cu nanopyramids by using the electrodeposition method in the presence of dodecylbenzene sulfonic acid sodium salt (DBSA), which acts as the stabilizer [23]. In this paper, we demonstrate that this approach can provide versatility in tuning the architectures, not only pyramidal but also cubic and multipod, of Cu particles on the surface of a polished Au substrate by systematically exploring the experimental parameters. To our knowledge, this is also the first report of the successful observation of the growth evolution of pyramidal NPs. This research is important for studying and understanding the growth mechanism of metal NPs with controllable shapes. These observations can be used not only for integration with advances in the creation of new nanoscale inorganic building blocks but also for their functional assemblies on crystallization processes.

Experimental Methods

Materials

Milli-Q water (18 MΩ resistivity; Millipore System) was used in all the experiments. Copper(II) tetrafluoroborate hydrate ($Cu(BF_4)_2 \cdot xH_2O$), dodecylbenzene sulfonic acid sodium salt, and poly(vinylpyrrolidone) (PVP) were purchased from commercial suppliers (Aldrich, Fluka, and Arcos, respectively). All the chemicals were used as received without further purification. Au films with 99.999% purity were supplied by Leesan Precious Metal Co., Ltd.

Synthesis of Cu NPs with Pyramidal, Cubic, and Multipod Shape

All the results reported here were obtained by using the basal planes of Au substrates that were cleaned in mixtures of 30% H_2O_2 and 98% H_2SO_4 (3:1 by volume) at 85 °C for 5 min (note that the mixture is dangerous since it reacts violently with organics) and sonicated in ethanol/water. A solution containing copper ions was prepared from 0.029 g of Cu ion precursor and 0.087 g of DBSA (the weight ratio

of DBSA/Cu^{2+} is 3). Pyramidal Cu NPs were synthesized on a cleaned Au substrate by immersing it in this solution. Electrochemical treatments were performed using a CH Instruments 672A electrochemical system with a three-electrode system at room temperature. A cleaned Au substrate (1 cm × 0.5 cm) acts as the working electrode, a platinum wire acts as the counter electrode, and an Ag/AgCl (immersed in a 3 M KCl filling solution saturated with AgCl) acts as the reference electrode. The deposition potential was controlled over a range from −0.6 to −0.8 V at a scan rate of 0.05 V s^{-1} [23], and the deposition time was 800 s. After the deposition, the electrodes were rinsed with large amounts of Milli-Q water to remove the residual-capping reagent. Identical experimental procedures can be used to obtain cubic and multipod Cu NPs; for the former, the weight ratio of DBSA/Cu^{2+} must be reduced to 2, and for the latter, DBSA should be replaced with PVP.

Characterizations

The field-emission scanning electron microscopic (FESEM) images were obtained using the GEMINI-URTRA 55 field-emission microscope. The X-ray diffraction patterns (XRD patterns) were recorded from SWLS X-ray Powder Diffraction with 01C beamline at the National Synchrotron Radiation Research Center (NSRRC), Hsinchu, Taiwan. The angle of incidence and the wavelength of the X-rays were 0.5 and 0.77490 Å, respectively.

Results and Discussions

Figure 1a is the FESEM image of the product obtained in the presence of the DBSA surfactant when the weight ratio of the DBSA/Cu precursor was 3; here, high-yield (over 70%) pyramid-shaped Cu NPs can be observed. The detailed structural analysis of the Cu nanopyramid was characterized by XRD, as shown in Fig. 1b. The peaks located at the 2θ values of approximately 24.9, 35.7, and 42.0 are assigned to the Cu(200), Cu(220), and Cu(311) facets of face-centered cubic (fcc) Cu, respectively. Crystallographic planes of XRD patterns were indexed using Bragg's law ($2d\sin\theta = n\lambda$) in which the wavelength of X-rays were 0.77490 Å, as well as combined with those of the JCPDS database (Cu file code: 85-1326). The XRD analysis also revealed that the films have a strong Au (111) peak, while the other diffraction peaks of Au (200), Au (220), Au (311), Au (222), Au (400), and Au (420) are weak, indicating the Au substrate was primarily composed of domains with the (111) structure. This implies that the surface of the Au crystal film under study was a polycrystal with a {111} orientation plane.

Fig. 1 a FESEM image of Cu pyramids on gold substrates with the weight ratio DBSA/$Cu^{2+} = 3$. The deposition potential ranged from -0.6 to -0.8 V (vs. Ag/AgCl) at a scan rate of 0.05 V s^{-1} for 800 s. *Inset: scale bar = 200 nm.* **b** The X-ray diffraction (XRD) pattern of the as-produced Cu pyramids. **c** Growth procedure for pyramidal Cu NPs. *Scale bar:* 200 nm. **d** Evolutionary pyramidal-shaped Cu NPs growth pathways
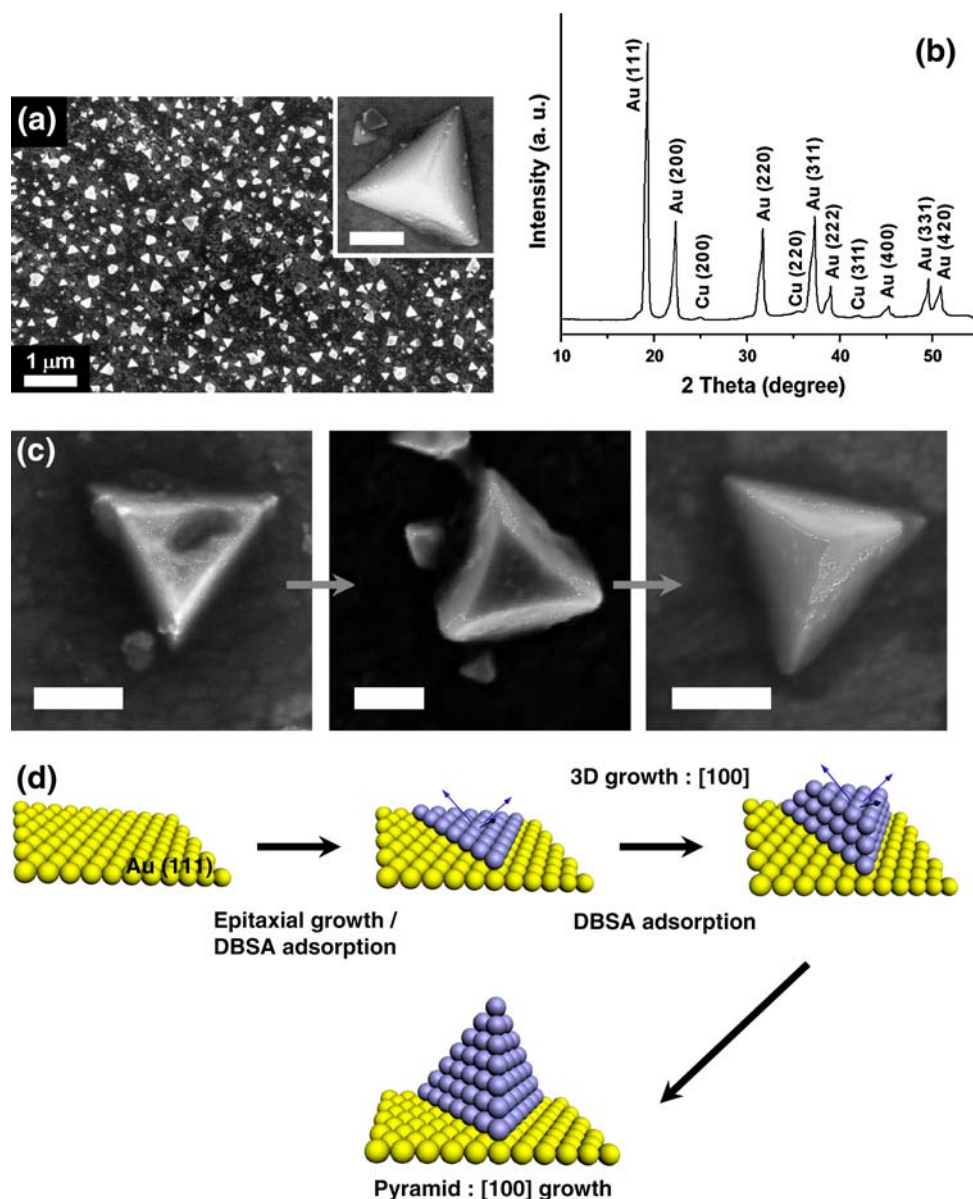
Interestingly, the growth sequence of metallic pyramids was also observed in the shape-control region for the first time (as shown in Fig. 1c); Cu NPs self-assembled into prism-shaped particles and finally into pyramids. It is commonly accepted that the shape of *fcc* nanocrystals is primarily determined by the ratio (R) of the growth rate along the [100] to that along the [111] direction [24, 25]. The balance between the two directions can be controlled kinetically, and the preferential capping or stabilization of some crystal faces by a surfactant can be used to change the growth kinetics and relative stability of the crystal faces in order to form the desired particle architecture; this phenomenon has also been reported for the shape control of Au and Ag NPs [26, 27]. Moreover, the growth of particles on substrates is epitaxially aligned with the crystal structure of the substrate surface, which leads to an epitaxial ordering

of deposited nanocrystals with the periodicity of the crystal structure of the substrate surface [28]. Therefore, the substrate selection can be regarded as another parameter for the formation of the pyramids. For comparison, the electrodeposition of Cu on indium tin oxide (ITO) was also performed. Only spherical but slightly faceted Cu NPs were noticed on the ITO (Figure S1). Combining the statements mentioned earlier, we assume that the growth sequence of Cu pyramids with the relative abundance of {111} facets can be explained as follows: At the initial stage of the deposition, Cu atoms epitaxially electrodeposit onto the (111) domains of Au surfaces, where DBSA does not participate in the electrochemical process but adsorbs onto some surfaces of the deposited Cu, thereby forming the first (111) plane of pyramid-shaped nanocrystals. Subsequently, the surface-regulating capping agent of

Fig. 2 Pyramidal, cubical, and multipod Cu particles deposited on gold substrates by using DBSA and PVP as the capping reagents. The *top* (**a**, **b**) FESEM images of the as-produced Cu NPs were prepared from the solution containing the weight ratios of DBSA/Cu^{2+} of 3 and 2, respectively. The *bottom* images represent the use of PVP as the capping agent. The deposition potential ranged from −0.6 to −0.8 V (vs. Ag/AgCl), the scan rate is 0.05 V s^{-1}, and the deposition time is 800 s
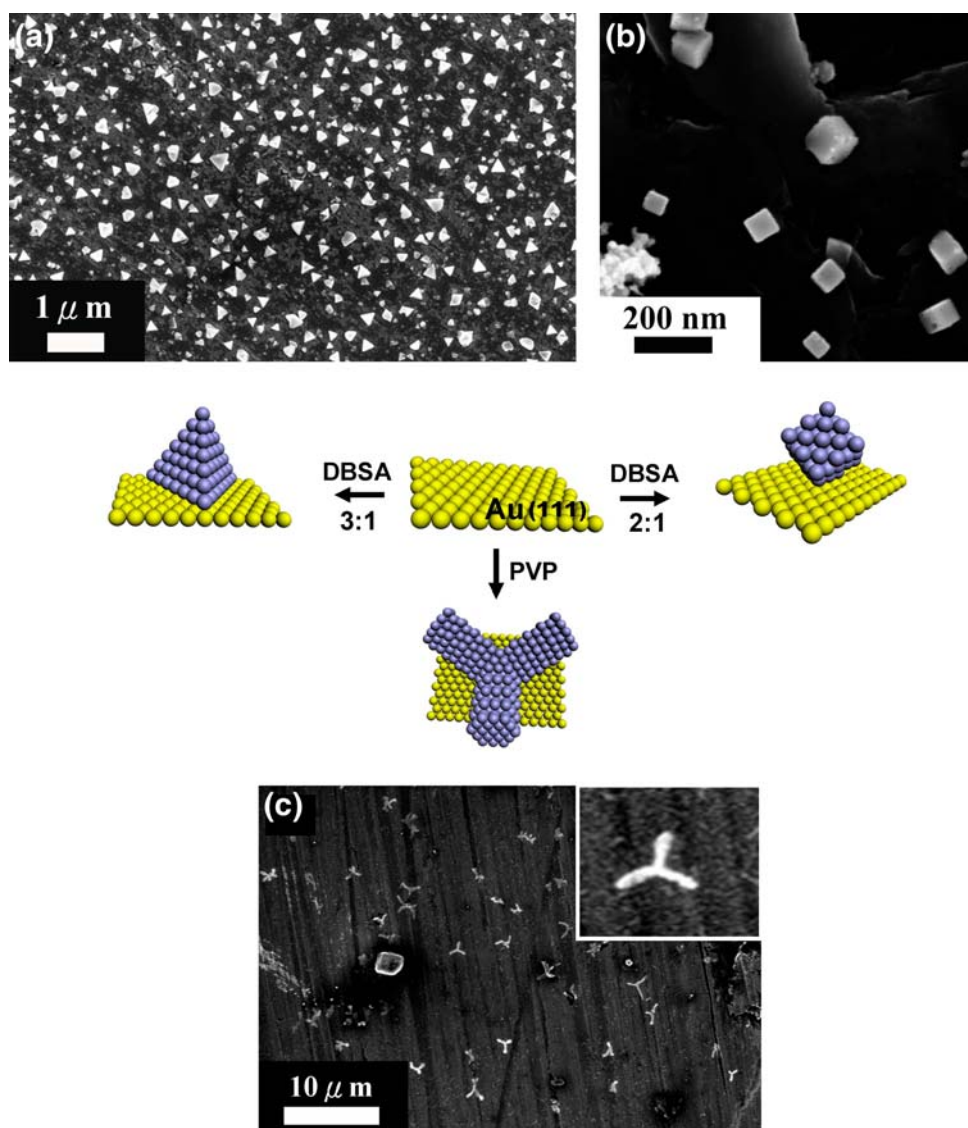
DBSA plays a critical role as the reaction proceeds, which results in stronger interactions with the atoms on the {111} facets than those on the {100} facets, leading to the preferential addition of Cu atoms onto the {100} facets [29]. This results in the enhancement of the growth rate along the [100] direction and/or reduction in the growth rate along the [111] direction, and ultimately, in the formation of pyramid-shaped Cu NPs. The scheme of the formation mechanism of a pyramidal Cu is shown in Fig. 1d.

It is commonly accepted that controlling the shape and structural architecture of metal NPs requires manipulation of the interplay between the faceting tendency of the stabilizing agent and growth kinetics. In the presence of capping reagents, the differences in the adsorption of surfactant/polymers on various crystal surfaces leads to a competitive growth, which results in shape variation. Therefore, the architectures of the Cu NPs should be varied depending on the concentrations and nature of the capping

agents. Under similar experimental conditions, cube-shaped Cu NPs were obtained when the weight ratio of DBSA/Cu^{2+} was decreased to 2. Figure 2 shows that the morphology of Cu NPs varies significantly with the amount of DBSA. This implies that decreasing the concentration of the capping agent DBSA might significantly influence the relative growth rates between the [111] and [100] directions, which would, in turn, affect the formation of the initial crystal seeds and the sequential growth of Cu NPs. Further, this ultimately leads to shape variations. Multipod Cu particles were unexpectedly found when the PVP polymer was used in place of DBSA, as shown in Fig. 2. PVP is believed to bind preferentially to the {100} and {111} planes [30], which induces the selective interaction and/or interaction strengths between PVP and the crystallographic facets of a Cu lattice; this behavior is substantially different from what is obtained when DBSA is used as the capping reagent. Hence, the early-stage nuclei and

sequential growth of deposited Cu atoms may be affected, which possibly leads onto the generation of a zinc blende-phased core with {111} planes followed by the growth of wurtzite-phased arms [31]. Finally, the formation of multipod Cu is induced. Further studies on the mechanism of Cu multipod formation are being performed.

Conclusions

From the researches conducted, which have been reported in this paper, we can summarize some main conclusions and their significance for the future development of related fields as follows:

1. Our electrodeposition method is a facile and versatile pathway for preparing high-yield pyramidal Cu NPs.
2. By using the controllable capping reagents DBSA and PVP, the electrodeposition method can be used to fabricate Cu particles having cubic and multipod shapes.
3. The growth evolution of pyramidal Cu NPs with a face-centered cubic (*fcc*) structure was also investigated for the first time; Cu NPs self-assembled into prism-shaped particles and finally into pyramids.
4. Our electrodeposition approach offers an economically attractive route toward broader applications for the formation of common transition group metals in the form of novel architectures, which can provide a powerful toolbox for applications such as biosensors, catalysis, fuel cells, and electronic nanodevices.

References

1. B. Wiley, Y.G. Sun, B. Mayers, Y.N. Xia, Chem. Eur. J. **11**, 454 (2005)
2. F. Kim, S. Connor, H. Song, T. Kuykendall, P.D. Yang, Angew. Chem. Int. Ed. **43**, 3673 (2004)
3. G.S. Metraux, C.A. Mirkin, Adv. Mater. **17**, 412 (2005)
4. C. Xue, Z. Li, C.A. Mirkin, Small **1**, 513 (2005)
5. S.S. Shankar, A. Rai, B. Ankamwar, A. Singh, A. Ahmad, M. Sastry, Nat. Mater. **3**, 482 (2004)
6. H. Lee, S.E. Habas, S. Kweskin, D. Butcher, G.A. Somorjai, P.D. Yang, Angew. Chem. Int. Ed. **45**, 7824 (2006)
7. M. Grzelczak, J. Perez-Juste, P. Mulvaney, L.M. Liz-Marzan, Chem. Soc. Rev. **37**, 1783 (2008)
8. C. Li, Z. Wang, P.I. Wang, Y. Peles, N. Koratkar, G.P. Peterson, Small **4**, 1084 (2008)
9. Y. Lee, J.R. Choi, K.J. Lee, N.E. Stott, D. Kim, Nanotechnology **19**, 415604 (2008)
10. J.G. Yang, T. Okamoto, R. Ichino, T. Bessho, S. Satake, M. Okido, Chem. Lett. **35**, 648 (2006)
11. J.G. Yang, Y.L. Zhou, T. Okamoto, T. Bessho, S. Satake, R. Ichino, M. Okido, Chem. Lett. **35**, 1190 (2006)
12. Y. Chang, M.L. Lye, H.C. Zeng, Langmuir **21**, 3746 (2005)
13. Y.H. Kim, Y.S. Kang, W.J. Lee, B.G. Jo, J.H. Jong, Mol. Cryst. Liquid Cryst. **445**, 231 (2006)
14. T. Nakamura, Y. Tsukahara, T. Sakata, H. Mori, Y. Kanbe, H. Bessho, Y. Wada, Bull. Chem. Soc. Jpn **80**, 224 (2007)
15. Y.H. Wang, P.L. Chen, M.H. Liu, Nanotechnology **17**, 6000 (2006)
16. E. Ramirez, L. Erades, K. Philippot, P. Lecante, B. Chaudret, Adv. Funct. Mater. **17**, 2219 (2007)
17. N.A. Luechinger, E.K. Athanassion, W.J. Stark, Nanotechnology **19**, 445201 (2008)
18. Z.L. Xiao, C.Y. Han, W.K. Kwok, H.H. Wang, U. Welp, J. Wang, G.W. Crabtree, J. Am. Chem. Soc. **126**, 2316 (2004)
19. K.S. Choi, Dalton Trans. **40**, 5432 (2008)
20. C.M. Lopez, K.S. Choi, Langmuir **22**, 10625 (2006)
21. N.D. Nikolic, K.I. Popov, L.J. Pavlovic, M.G. Pavlovic, Surf. Coat. Technol. **201**, 560 (2006)
22. S. Kumar, S.K. Chakarvarti, Dig. J. Nanomat. Biostruct. **1**, 139 (2006)
23. W.Y. Ko, W.H. Chen, S.D. Tzeng, S. Gwo, K.J. Lin, Chem. Mat. **18**, 6097 (2006)
24. Z.L. Wang, J. Phys. Chem. B **104**, 1153 (2000)
25. J.M. Petroski, Z.L. Wang, T.C. Green, M.A. El-Sayed, J. Phys. Chem. B **102**, 3316 (1998)
26. Y.G. Sun, B. Mayers, T. Herricks, Y.N. Xia, Nano Lett. **3**, 955 (2003)
27. Y.G. Sun, Y.N. Xia, Science **298**, 2176 (2002)
28. S. Gorer, J.A. Ganske, J.C. Hemminger, R.M. Penner, J. Am. Chem. Soc. **120**, 9584 (1998)
29. Z.P. Qiao, Y. Zhang, L.T. Zhou, Q.C. Xire, Cryst. Growth Des. **7**, 2394 (2007)
30. A.R. Tao, S. Habas, P.D. Yang, Small **4**, 310 (2008)
31. S.H. Chen, Z.L. Wang, J. Ballato, S.H. Foulger, D.L. Carroll, J. Am. Chem. Soc. **125**, 16186 (2003)